Journal of Biomedical Optics

SPIEDigitalLibrary.org/jbo

Filter-based method for background removal in high-sensitivity wide-field-surface-enhanced Raman scattering imaging *in vivo*

Rupananda J. Mallia
Patrick Z. McVeigh
Israel Veilleux
Brian C. Wilson

SPIE

TECHNICAL NOTE

Filter-based method for background removal in high-sensitivity wide-field-surface-enhanced Raman scattering imaging *in vivo*

Rupananda J. Mallia,[a*] Patrick Z. McVeigh,[b*] Israel Veilleux,[a] and Brian C. Wilson[a,b,c]
[a]University Health Network, Ontario Cancer Institute, Toronto, Ontario, Canada
[b]University of Toronto, Department of Medical Biophysics, Toronto, Ontario, Canada
[c]University Health Network, Techna Institute, Toronto, Ontario, Canada

Abstract. As molecular imaging moves towards lower detection limits, the elimination of endogenous background signals becomes imperative. We present a facile background-suppression technique that specifically segregates the signal from surface-enhanced Raman scattering (SERS)-active nanoparticles (NPs) from the tissue autofluorescence background *in vivo*. SERS NPs have extremely narrow spectral peaks that do not overlap significantly with endogenous Raman signals. This can be exploited, using specific narrow-band filters, to image picomolar (pM) concentrations of NPs against a broad tissue autofluorescence background in wide-field mode, with short integration times that compare favorably with point-by-point mapping typically used in SERS imaging. This advance will facilitate the potential applications of SERS NPs as contrast agents in wide-field multiplexed biomarker-targeted imaging *in vivo*. [DOI: 10.1117/1.JBO.17.7.076017]

Keywords: surface-enhanced Raman scattering; molecular imaging; gold nanoparticles; tissue fluorescence; *in vivo* imaging; wide-field Raman.

Paper 12180TN received Mar. 15, 2012; revised manuscript received May 15, 2012; accepted for publication May 17, 2012; published online Jul. 13, 2012.

1 Introduction

Molecular imaging of various forms, based on both optical and non-optical signals, is evolving rapidly, not only in terms of the range of potential biomarkers for targeting contrast agents, but also in the variety of these agents and corresponding imaging techniques and instruments, for both preclinical research and clinical applications.[1] Optical nanoparticle (NP)-based contrast agents, including fluorescent quantum dots (QD) and surface-enhanced Raman scattering (SERS)-active NPs, have been a focus of recent research.[2,3] The latter comprises of a metal core coated with a "reporter" molecule that has a distinct SERS spectral signature. Although QDs have marked photophysical advantages over organic fluorophores as imaging probes (photostability, broad excitation spectra, and higher multiplexing capability),[4] their applicability *in vivo* has, to date, been limited by their relatively inefficient excitation in the near infrared (NIR) region where tissue autofluorescence is minimized, potential heavy metal toxicity and fluorescence intermittency (blinking).[4–6] SERS-active NPs based on colloidal gold cores address these shortcomings, including specifically the first two, and the amplification of the Raman signal from the reporter molecule(s) on the surface of metal nanoparticles (due to plasmonic effects) may be high enough ($>10^6$-fold) to make them competitive with fluorophores in terms of the optical signal strength.[5]

If comparable, or at least useful, SERS signal strength can be realized, and then advantage of the extremely narrow (~1 to 3 nm) spectral features becomes very important compared with organic fluorophores or even quantum dots to enable high level multiplexing,[7] as illustrated in Fig. 1. For instance, it is increasingly clear that the targeting of tumors with high specificity for personalized cancer medicine will require simultaneous targeting of multiple (likely >5) biomarkers,[6,7] because of high inter-patient heterogeneity in the expression profiles. Thus, an effective contrast agent will require a "cocktail" of reporters that can be cleanly separated spectrally for effective multiplexing. In addition, the colloidal core size and optical absorption spectra of reporter molecules on SERS NPs can be selected to provide highly efficient excitation and detection in the 750 to 900 nm ("optical window") region where background tissue absorption and fluorescence are minimal, improving both the *in vivo* probe sensitivity and depth of detection. In practice, however, SERS NPs are always used at significantly lower concentrations than fluorophores, due primarily to the cost. This negates much of the signal-to-background advantage, since the SERS signal is then typically only a small perturbation ($\ll$5%) on the tissue autofluorescence background, as we show below.

SERS imaging is usually performed by full-spectrum raster scanning, point-by-point across the image, as, e.g., in confocal Raman microscopy.[8] In every pixel, each contributing Raman-active molecule can then be isolated, based on their unique Raman signatures, typically applying polynomial curve fitting to subtract the background spectrum. This requires long integration times to acquire sufficient signal-to-noise in each pixel across the field of view.[8,9] In the case of imaging the intrinsic NIR Raman signature of tissues or cells, the alternative would be to use an expensive focal plane array and a fast tunable filter. However, for imaging SERS contrast agents, since the location of the narrow SERS peaks of the reporter molecule(s) is known

*These authors contributed equally to this work.

Address all correspondence to: Brian C. Wilson, University Health Network, Ontario Cancer Institute, Toronto, Ontario, Canada. Tel: (416) 946-2952; Fax: (416) 946-6529; E-mail: wilson@uhnres.utoronto.ca

0091-3286/2012/$25.00 © 2012 SPIE

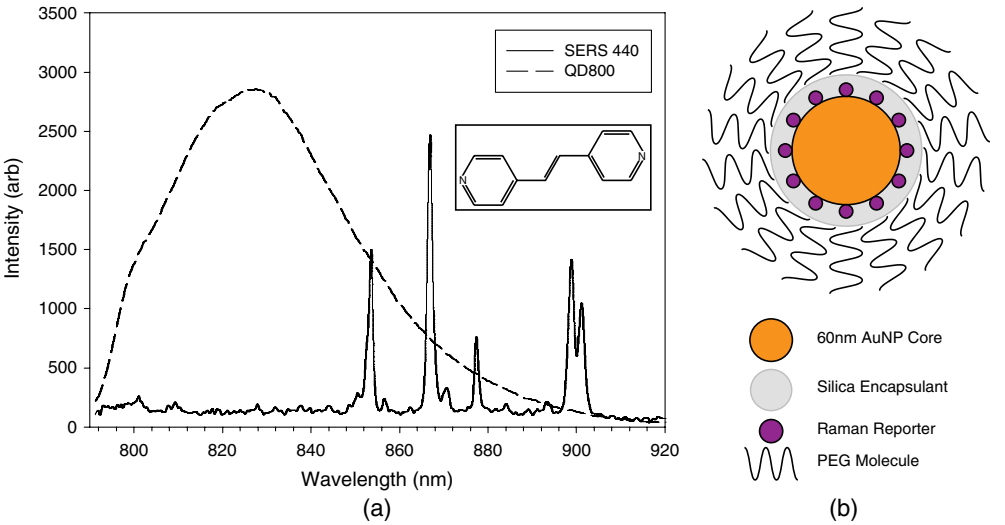

Fig. 1 (a) Comparison of the SERS spectrum from the S440 reporter molecule (inset) and 800-nm peak-emission quantum dots, both excited at 785 nm, and (b) schematic of SERS AuNPs with 60-nm colloidal gold core, adsorbed SERS reporter molecule, 30-nm thick silica encapsulant, and polyethylene glycol surface coating.

a priori, rapid background-free wide-field imaging should be possible using narrow-bandpass (BP) filters centered on these peaks. Then, for each peak, over sufficiently small spectral windows, all non-SERS contributions are approximately linear functions of wavenumber. Hence, the background can be accurately determined and subtracted by using narrrow BP filters immediately on each side of the SERS peak. Since this requires at most three images per SERS line of interest, the time to form a complete SERS contrast image is reduced by orders of magnitude over complete spectral mapping at equivalent optical resolution.[9] Here, we present a proof-of-principle demonstration of this approach.

2 Material and Methods

2.1 *SERS-Active Gold Nanoparticles*

SERS-active gold nanoparticles (AuNPs) were purchased from Cabot Security Materials Inc. (Mountain View, CA, USA) and consist of a 60-nm colloidal gold core, an adsorbed layer of the Raman-active molecule S440 [Trans-1,2-Bis(4-pyridyl)-ethylene],[7] and a 30-nm thick thiolated silica encapsulant layer that stabilizes the reporter molecule on the AuNP surface and provides a reactive substrate for further conjugation steps. For *in vivo* use, the AuNPs are further coated with polyethylene glycol (PEG) to improve their biostability. A schematic diagram of structure and the corresponding SERS spectrum are shown in Fig. 1. These NPs can be targeted by attaching suitable tumor specific agents, e.g., antibodies, affibodies, or peptides, to the silica, either directly or through flexible linker molecules.[5,10]

2.2 *Instrumentation and Image Processing*

Wide-field SERS BP imaging was performed using an instrument built in-house, comprised of a virtual-phase EM-CCD camera (Andor, Belfast, UK) with motorized interference filters to select the SERS bands of interest and to reject Rayleigh scattered light, together with suitable relay optics to provide a 2.2-cm diameter uniform field of view at a working distance of 15 cm. For the proof-of-principle studies, a single SERS line at 900 nm (1630 cm^{-1}) was selected. The corresponding BP filters (900, 910, and 890 nm) were selected to be relatively inexpensive and have a bandwidth of approximately 10 nm (FB10 series, Thorlabs, Newton, NJ, USA), with a peak transmission of *ca.* 50%. Excitation over a 1 cm area of the sample was provided by a 400 mW 785 nm fiber-coupled diode laser (BWTek, Newark, DE, USA), so that the power density was below the ANSI skin exposure limit for 3 s continuous-wave laser exposure.[8]

By considering a sufficiently narrow spectral window, we assume that the non-SERS background spectrum is a linear function of wavelength, so that in each image pixel it may be approximated by linear interpolation of the corresponding off-peak pixel intensities. Here, to simplify the procedure, we have used BP filters that have symmetric in-band transmission spectra, are equally spaced on either side of the SERS peak, and do not have significant spectral overlap, and have used a spectral range where the quantum efficiency of the detector is linear over the spectral window. However, the approach can easily be extended to the more general case by including appropriate scaling factors, if required.

2.3 *In Vivo Imaging*

All animal procedures were carried out under institutional approval (University Health Network, Toronto, Canada), using eight-week old female nude mice (Taconic, Hudson, NY, USA). The objective was to determine the lowest NP concentration that could be detected with the imaging system. Both SERS-active and control NPs without the S440 reporter molecule were used, at concentrations of 20 to 360 pM, and mixed 1 : 1 with Matrigel (BD, Mississauga, Ontario, Canada). Under general anesthesia, 10 μL of each concentration was injected subcutaneously at different locations along the dorsum of an individual mouse immediately prior to imaging.

3 Results and Discussion

Figure 2 shows a typical full-spectrum point measurement taken on a confocal Raman microscope with a 40 pM SERS AuNP sample placed on *ex vivo* mouse skin, showing the expected SERS signal superimposed on the broad tissue autofluorescence

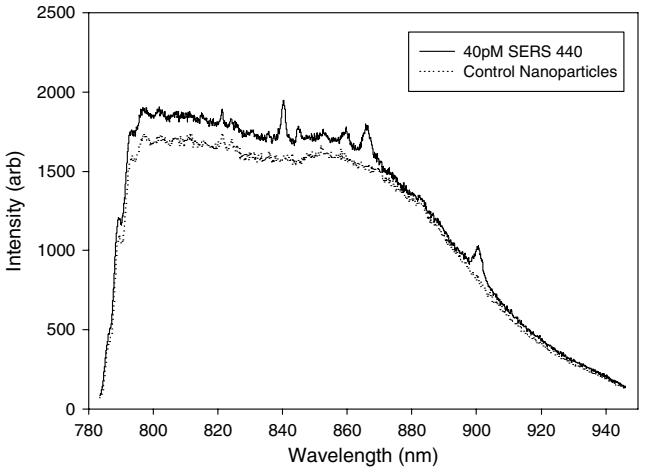

Fig. 2 Raman spectra of 40 pM control gold nanoparticles (no reporter molecule: dotted line) and SERS-active nanoparticles (solid line) measured on a background of *ex vivo* mouse skin; SERS signals are typically a small perturbation (≪5%) on the broad tissue background.

background. Even though the tissue autofluorescence is greatly reduced with NIR (785 nm) excitation compared to visible excitation,[11] it still overwhelms the SERS signal at these pM nanoparticle concentrations. In other *in vivo* point-spectroscopy studies of intrinsic tissue Raman, post-processing of the spectrum has often been used to subtract the autofluorescence background[12] but, as mentioned above, this cannot directly be applied in wide-field imaging mode.

Figure 3 shows BP images of a 40 pM sample taken at 900 nm (SERS peak) and the two adjacent wavelengths (890 and 910 nm). The on-peak image is not appreciably brighter than the adjacent off-peak images. Furthermore, this background varies significantly for every sample, depending on composition, illumination conditions, and acquisition parameters, so that it cannot simply be subtracted by calibration measurements.

Figure 4(a) shows the details of the 900 nm SERS peak and the 3 BP filters, while Fig. 4(b) shows images of SERS-active and control NPs on a non-tissue background. The image intensities are not significantly different when considering only the peak signal, even in this simple case. However, Fig. 4(c) and 4(d) shows significant enhancement of the signal-to-background ratio (SBR) in the SERS images (from 1.7 to 9.1) after applying the linear background subtraction, even at very short total exposure times.

The *in vivo* imaging test results are shown in Fig. 5; as expected, there was significant tissue autofluorescence that camouflaged the SERS signal, such that the lower NP concentrations were indistinguishable from control AuNPs in the single-band images. However, following the filter-based linear background removal, images with excellent SBRs (356 and 9.3 for 40 and 20 pM, respectively) could be acquired at low pM concentrations using image integration time of only a few seconds. Similar to QDs and other organic fluorophores, we observed an ultimate decrease in the limit of detection as a function of depth in tissue. However, the use of SERS nanoparticles excited in the NIR should give markedly greater *in vivo* penetration depth than QDs excited in the UV-visible range. It is also

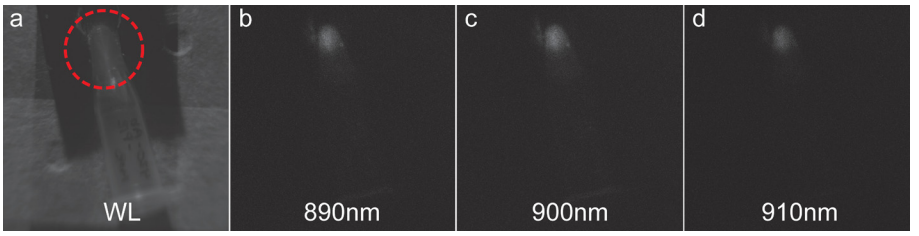

Fig. 3 SERS bandpass images of 40 pM SERS-active AuNPs in solution. (a) White light image showing the laser irradiation volume, and (b) to (d) SERS bandpass images centered at 890, 900, and 910 nm, respectively; excitation at 785 nm with 1 s integration time per image. Circle indicates the laser illumination spot.

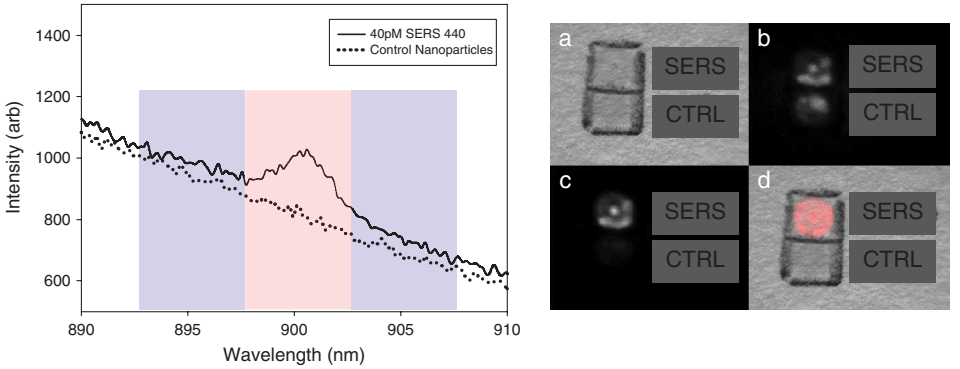

Fig. 4 (left) SERS spectrum illustrating the filter passbands used to isolate the SERS signal (solid) from background (dashed). (right) (a) white-light image of 40 pM SERS-active and control AuNPs on filter paper, (b) 900 nm image showing signal from both samples, (c) linear background-subtracted image demonstrating improved SBR (1.7 to 9.1), and (d) background-subtracted signal shown in fasle color superimposed on the white light image; excited simaltaneously at 785 nm with 1 s image integration.

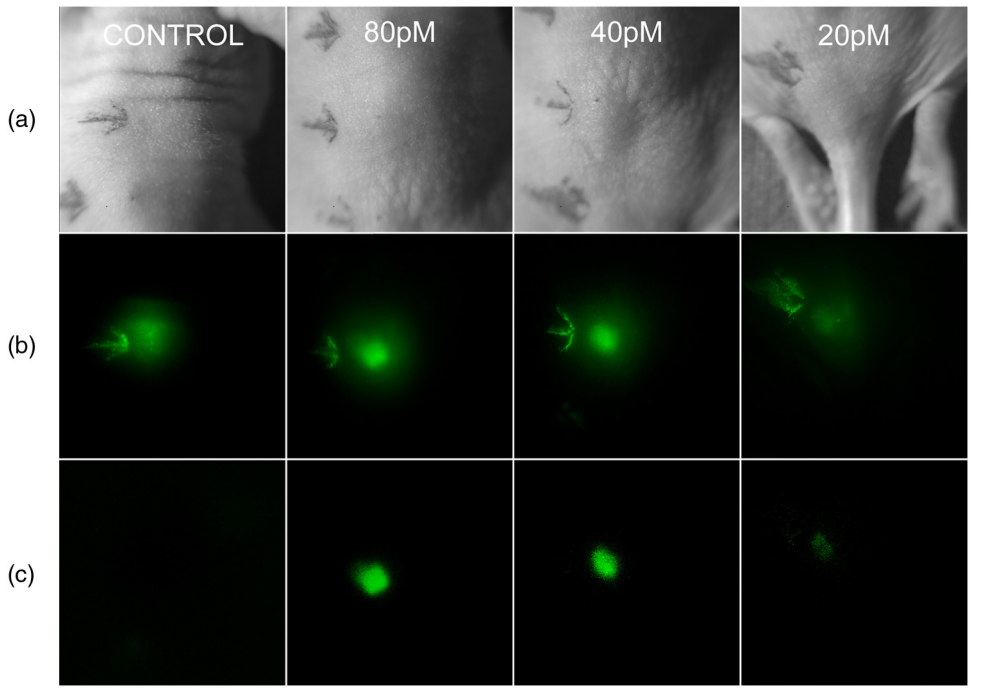

Fig. 5 *In vivo* imaging of SERS AuNPs subcutaneously at different concentrations in dorsal mouse skin: (a) white-light images, with arrows indicating AuNP injection sites; (b) 900-nm bandpass SERS images showing poor SBRs (1.1, 0.98, and 0.92 at 80, 40, and 20 pM, respectively); (c) background-subtracted images demonstrating improved SBRs (905, 356, and 9.3 at 80, 40 and 20 pM, respectively) and visualization even as low as 20 pM AuNPs; 785-nm excitation with 3 s image integration in all cases.

worth noting that, in the case of topically applied SERS AuNPs for endoscopic detection of early cancer,[10] the optical penetration depth is not likely to be the limiting factor, but rather the penetration of the NPs into the tissue.

From these results it is evident that this rapid imaging capability is critically important for translation, especially for clinical applications, where the typical point-by-point full-spectrum mapping to form SERS contrast images[7] can take minutes to hours for comparable spatial resolution. Thus, for example, at a working distance of 120 mm, our system has an approximate CCD pixel resolution of 25 μm and required 9 s to acquire the three BP images for a 1 cm diameter illumination spot, whereas point-by-point spectral scanning with equal integration time per pixel and spatial resolution would require in excess of 125 h.

Currently, the main limitations of this technique are the time delay for filter switching and the relatively broad transmission profile of the filters used, which limits the achievable level of multiplexing. In practical terms, the degree of achievable multiplexing depends partly on the spacing between peaks of the different SERS reporter molecules selected. If major peaks between the reporter molecules are spectrally isolated, i.e., the spectra do not interfere, then the detection limit should be similar to that demonstrated here. If there is spectral overlap even with the best reporters available, then there will be loss of sensitivity. In such cases, it will likely be necessary to apply a more rigorous linear spectral-unmixing algorithm, as we have used previously in hyperspectral fluorescence imaging.[13] We are currently investigating this for SERS imaging, using multiple discrete BP filter bands for each reporter. We are also currently implementing a modified version of the instrument, using a fast tuneable narrow BP filter with high transmission efficiency. This should both further reduce the total imaging time and allow programmable multiplexed imaging to match any "cocktail" of selected SERS reporters.

4 Conclusions

In summary, we have shown that a simple and economical filter-based technique can markedly reduce the intrinsic background signals in wide-field SERS imaging, enabling fast imaging with pM nanoparticle sensitivity, which is below the typical AuNP concentrations reported *in vivo* to date.[5,7] The proof-of-concept results clearly demonstrate significant improvement in the signal-to-background ratio as compared to direct SERS peak imaging at biologically realistic AuNP concentrations. The approach could also be extended to image other SERS bands of interest for multiplex imaging by appropriately selecting additional discrete filters or by using a single tunable filter. This background suppression approach should facilitate the further development and deployment of SERS-based contrast agents for prospective molecular imaging *in vivo*. Capitalizing on this pragmatic technique, development of a wide-field endoscopic imaging system is also underway.

Acknowledgments

Funding was provided by the NSERC Strategic Network for Bioplasmonic Systems (BiopSys). P.Z.M. is also supported by a Vanier Scholarship from the Canadian Institutes of Health Research.

References

1. K. K. Jain, "Nanomedicine: application of nanobiotechnology in medical practice," *Med. Princ. Pract.* **17**(2), 89–101 (2008).
2. K. K. Jain, "Recent advances in nanooncology," *Technol. Cancer. Res. Treat.* **7**(1), 1–13 (2008).

3. K. B. Hartman, L. J. Wilson, and M. G. Rosenblum, "Detecting and treating cancer with nanotechnology," *Mol. Diagn. Ther.* **12**(1), 1–14 (2008).
4. I. L. Medintz, H. Mattoussi, and A. R. Clapp, "Potential clinical applications of quantum dots," *Int. J. Nanomedicine* **3**(2), 151–167 (2008).
5. X. Qian et al., "In vivo tumor targeting and spectroscopic detection with surface-enhanced Raman nanoparticle tags," *Nature Biotechnol.* **26**(1), 83–90 (2009).
6. S. Nie and S. R. Emory, "Probing single molecules and single nanoparticles by surface enhanced Raman scattering," *Science* **275**(5303), 1102–1106 (1997).
7. C. L. Zavaleta et al., "Multiplexed imaging of surface enhanced Raman scattering nanotags in living mice using noninvasive Raman spectroscopy," *Proc. Natl. Acad. Sci. U.S.A.* **106**(32), 13511–13516 (2009).
8. S. Keren et al., "Noninvasive molecular imaging of small living subjects using Raman spectroscopy," *Proc. Natl. Acad. Sci. U.S.A.* **105**(15), 5844–5849 (2008).
9. S. Schlucker et al., "Raman microspectroscopy: a comparison of point, line and wide-field imaging methodologies," *Anal. Chem.* **75**(16), 4312–4318 (2003).
10. J. V. Jokerst et al., "Affibody-functionalized gold–silica nanoparticles for Raman molecular imaging of the epidermal growth factor receptor," *Small* **7**(5), 625–633 (2011).
11. C. J. Frank et al., "Raman spectroscopy of normal and diseased human breast tissue," *Anal. Chem.* **67**(5), 77–783 (1995).
12. J. Zhao et al., "Automated autofluorescence background subtraction algorithm for biomedical Raman spectroscopy," *Appl. Spectroscopy* **61**(11), 1225–1232 (2007).
13. P. Constantinou, R. R. DaCosta, and B. C. Wilson, "Extending immunofluorescence detection limits in whole paraffin-embedded formalin fixed tissues using hyperspectral confocal fluorescence microscopy," *J. Microscopy* **234**(2), 137–146 (2009).